

## Influence of Nonlinear Behavior of Pile-Soil Structure on Displacement Amplitude Dependence for Efficiency of Pile Group Based on Cyclic Lateral Loading Tests Subjected to Large Displacement Amplitude

H. KASHIWA<sup>1</sup>, M. SHOUJI<sup>1</sup>, Y. HAYASHI<sup>2</sup>, K. SUITA<sup>3</sup>, T. KURATA<sup>4</sup> and W. INOUE<sup>1</sup>

<sup>1</sup> Graduate Student, Dept. of Architecture and Architectural Eng., Kyoto Univ., Kyoto, Japan

<sup>2</sup> Prof., Dept. of Architecture and Architectural Eng., Kyoto Univ., Kyoto, Japan

<sup>3</sup> Assoc. Prof., Dept. of Architecture and Architectural Eng., Kyoto Univ., Kyoto, Japan

<sup>4</sup> Nippon Steel Engineering, Tokyo, Japan

Email: kashiwamochi@t24y0230.mbox.media.kyoto-u.ac.jp

### ABSTRACT :

The cyclic lateral loading tests for the pile group in dry sand subjected extremely large displacement were conducted to investigate the mechanism of the strong nonlinear behavior of pile-soil structures which is not considered in Japanese seismic design. Furthermore, elastic-plastic 3-D finite element analyses, in which the pile and the soil were assumed to have the plastic characteristics and the contact boundary condition was considered between the pile and the soil, were performed to obtain better understanding of the tests results. In this paper, the applicability of 3-D finite element analyses is presented by comparing the calculated analysis results with the observed test results, and then the influence of the nonlinear behavior of the pile-soil structure on the amplitude dependency of the effect of pile groups is discussed by parametric study with 3-D finite element analyses. It is shown that the analyses can simulate the lateral resistance behavior of pile groups by taking the material nonlinearity of the pile and the soil into account.

### KEYWORDS:

Lateral resistance of pile; Strong nonlinearity  
Pile group efficiency; Finite element method

### 1. INTRODUCTION

The near-fault ground motions observed in Kobe and Niigata Chuetsu Earthquakes is far stronger than those commonly used for the Japanese seismic design. The strong nonlinear behavior of pile-soil structures, which is the separation between the pile and the soil, the slip in the soil or the yielding of the pile cap, will occur under the strong ground motions, and will significantly affect the lateral resistance of piles. To perform the seismic design rationally, the strong nonlinear behavior of pile-soil structures should be accurately considered. Therefore, the mechanism of the strong nonlinear behavior should be investigated.

The lateral resistance of pile groups is complex and much attention has been paid to this problem. For instance, vibration tests of pile-supported structure in liquefiable sand using large-scale blast by Saito et al. (2002), lateral loading tests of pile group in sand by Brown et al. (1988), horizontal loading tests to investigate the characteristics of subgrade reaction of pile group by Suzuki et al. (2003), experimental studies on lateral behavior of pile groups under combined load by Tominaga et al. (1988).

Many researches have dealt with the pile group effects. However, few studies have been reported on the pile group effects with the strong nonlinear behavior of pile-soil structures. To investigate the mechanism of the strong nonlinear behavior of pile-soil structures which is not considered in current seismic design, the test results should be accumulated. Therefore, the cyclic lateral loading tests for the pile group in dry sand subjected extremely large displacement were conducted. Furthermore, elastic-plastic 3-D finite element analyses, in which the pile and the soil were assumed to have the plastic characteristics and the contact boundary condition was considered between the pile and the soil, were performed to obtain better understanding of the tests results. In this paper, the applicability of 3-D finite element analyses is indicated by comparing the calculated analysis results with the observed test results, and then the influence of the nonlinear behavior of pile-soil structure on

the amplitude dependency of the effect of pile groups is discussed by parametric study with 3-D finite element analyses.

## 2. LATERAL LOADING TEST

### 2.1. Test Setup

Figure 1 show a setup of the test apparatus used for the 2-by-2 pile group loading test. The tests were conducted in a rectangular rigid tank 3000mm × 1200mm × 1000mm. The piles was set in sand to a depth of 830mm and laterally loaded at 170mm from the soil surface. The test apparatus was designed to load piles through a rigid loading frame. The pile caps were fixed to the rigid loading frame with high strength bolts and the pile ends were free. The rigid loading frame was supported by the guide rollers, which had low friction, and was restricted so that it was able to move linearly in one direction. The hydraulic actuator is used for loading and the tests were conducted with the gradually increasing displacement amplitudes. The target amplitudes  $\delta$  normalized by the pile diameter  $B$  adopted for tests were 0.017 $B$ , 0.033 $B$ , 0.067 $B$ , 0.1 $B$ , 0.13 $B$ , 0.17 $B$ , 0.2 $B$ , 0.25 $B$ , 0.3 $B$ , 0.4 $B$ , 0.5 $B$ , 0.75 $B$ , and 1.0 $B$  for all the cases. For each amplitude, loading was repeated for two cycles.

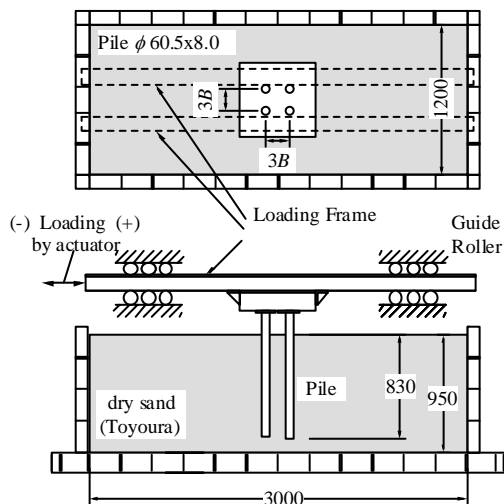


Figure 1 Setup of test apparatus

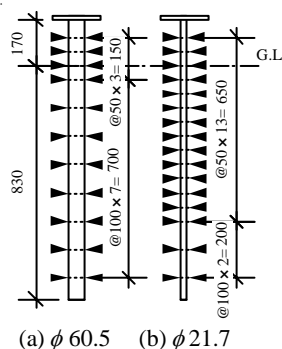

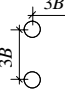
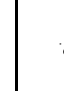
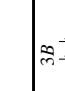
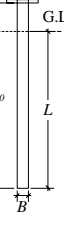
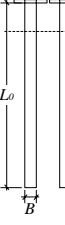

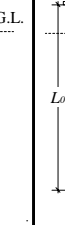


Figure 2 Pile specimen and location of strain gage

Table 1 Test case

Test name	1P	4P	1P-S	4P-S
Number of pile	1	4	1	4
Diameter $B$ (mm)	60.5	60.5	21.7	21.7
Length $L_0$ (mm)	1000	1000	1000	1000
Length in soil $L$ (mm)	830	830	830	830
Relative density (%)	60	61	65	63
Plan				
Shape of pile				

As shown in Table 1, the model tests for several cases of the single pile and the 2-by-2 pile group were prepared by two different kinds of piles, i.e., one was the short pile named as 1P, 4P and the other was the slender pile named as 1P-S, 4P-S. The piles were steel pipes (STK400). The short pile had 60.5mm outer diameter and 8mm thickness and the slender pile had 21.7mm outer diameter and 1.9mm thickness. The yield stress of the short

pile was 295N/mm<sup>2</sup>, the yield moment was 4.54kN · m and the full plastic moment was 6.56kN · m. The yield stress of the slender pile was 373N/mm<sup>2</sup>, the yield moment was 0.20kN · m and the full plastic moment was 0.27kN · m. By 'Recommendations for Design of Building Foundations', piles are classified into two groups as lateral deflections, one is the infinitely long member and the other is the infinitely short member. 'Recommendations for Design of Building Foundations' suggests the following expression for the infinitely long member:

$$\beta L > 2.25 \quad (1)$$

where  $\beta = \{k_h \cdot B / (4K)\}^{1/4}$  (1/m),  $L$ =length of pile in the soil (m),  $k_h$ =coefficient of horizontal subgrade reaction at  $0.3B$  (kN/m<sup>3</sup>),  $K$ =flexural rigidity of pile (kN · m<sup>2</sup>). The value of  $\beta L$  of the short pile was 1.01 and that of the slender pile was 2.33, so that the short pile was classified into the infinitely short pile and the slender pile was classified into the long pile. In the pile group tests, the pile spacing was  $3B$ . The model soil was consisted of Toyoura sand. The specific gravity, the maximum void ratio, and the minimum void ratio of Toyoura sand are 2.65, 0.95, and 0.58, respectively. The model soil preparation was summarized as follows: 1) The layered soil segmented into 10 layers was put in the tank softly by using the container bag carried by crane. The layered soil was consisted of nine layers of 100mm depth and one layer of 50mm depth. 2) The surface of each layered soil was smoothed by using a trowel and compacted by using a vibrator. 3) The depth of the layered soil was verified by the distance from the top of the test tank to the soil surface to control the relative density of the layered soil was calculated.

Figure 2 shows the details of the instrumentation. The piles were instrumented with strain gauges. The bending moment and the shear force were estimated by the bending component of axial strain measured by strain gauges. The total lateral load at the top of piles was measured by a load cell attached to the hydraulic actuator.

## 2.2. Test Result (Ground Deformation)

Plan and section views of ground deformation for 1P, 4P, 1P-S and 4P-S are shown in Figure 3. Furthermore, the pictures of the ground deformation for 4P are shown in Figure 4. The solid lines show the shape of the surface of the ground around piles, and broken lines are the traces of the ground slip.

In all cases, it could be observed that the ground outside the pile or the pile group was deformed like a corn shaped hollow. The process of this deformation observed during the tests are as follows; 1) The sand behind the pile settled down as the pile moved and then the ground behind the pile was deformed like a corn shaped hollow. 2) As the pile was loaded repeatedly, the corn shaped hollow was formed in both loading direction. The diameter and the depth of the hollow expanded as displacement amplitude increase.

As shown in Figure 4(a), it is clear that the ground outside the pile group was deformed significantly like a corn shaped hollow, whereas the ground inside the pile group was deformed less and kept the shape like a small hill. The height of this small hill decreased with increasing displacement amplitude. The behavior of the ground deformation observed for 4P can also be seen in the results of 4P-S. When the amplitude reached  $0.3B$ , a deformation line occurred on the ground surface between two piles as shown in Figure 4(b). This deformation line was due to the slip between the ground in front of the trailing pile and the ground around the trailing pile. The ground inside the deformation line moved together with the piles.

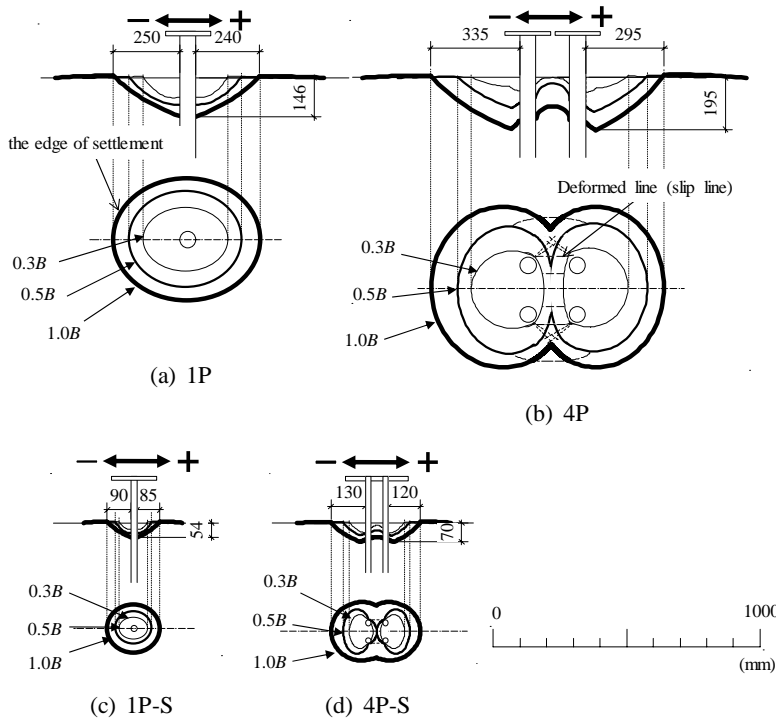
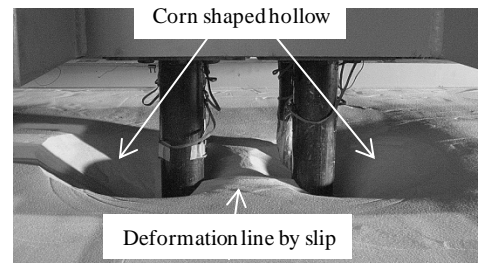
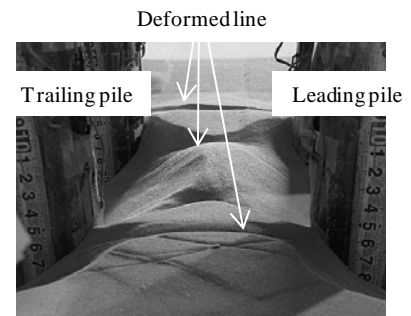


Figure 3 Plan and section view of ground



(a) Around the pile group



(b) Deformation line (slip line)

Figure 4 Ground deformation ( $\delta/B=0.3$ )

### 3. TEST SIMULATION BY 3D FINITE ELEMENT ANALYSIS

The 3-D finite element analyses were conducted to simulate the test results and to investigate the influence of nonlinearity of the pile-soil structure on the pile group effect.

#### 3.1. 3D Finite Element Model

Figure 5 shows the finite element mesh for 4P. The size of the model was same as that of the test apparatus. The sides and bottom of the model of soil were fixed in all three coordinate directions with the exception of the symmetric boundary, which was only supported in the direction perpendicular to the symmetry plane. The contact condition, which allowed the slip and the separation of the contacting surfaces, was applied between the pile and the soil. The pile caps were fixed in all rotated coordinate directions and were subjected monotonic displacement in one direction. The bottom edges of piles were free. The analyses were controlled by the horizontal displacement of the pile cap.

The material properties used in the analyses are summarized in Table 2. The pile was assumed to be an elastic-plastic constitutive model with coefficient of strain hardening  $e_t$  and yield stress  $\sigma_y$ , which was obtained from the uniaxial compression material testing. The soil was assumed to be a Mohr-Coulomb elastic-plastic constitutive model with no associated flow rule. The values of material properties of the soil in the analyses were determined from the previous researches which conducted similar analyses. The Young's module  $E_s$  of the soil was the average value from the ground surface to the depth of the pile end to be given by the following equation by Wakai et al (1999):

$$E_s = E_{50} = E_0 (p/p_0)^{0.5} \quad (2)$$

where  $E_{50}$  = the secant elastic module ( $\text{kN/m}^2$ ),  $E_0 = 19.6 \text{ MPa}$ ,  $p_0 = 98 \text{ kPa}$ ,  $p$  = the mean effective normal stress (kPa). The soil was assumed to have very small cohesion to improve the convergence of this analysis. The friction angle  $\phi$  of the soil was 40 degree (e.g., Tatsuoka et al, 1986). The dilation angle  $\psi$  was assumed to be

given by  $\psi = \phi - 30$  (e.g., Tatsuoka, 1993).

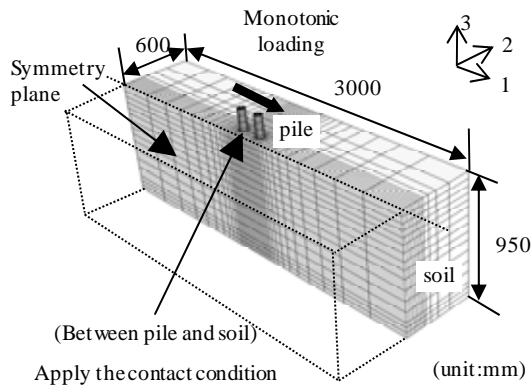


Figure 5 Layout of 3D meshes for FEM

Table 2 Material properties used in the analysis

Pile	Yield stress $\sigma_y$ (N/mm <sup>2</sup> )	370
	Coefficient of strain hardening $e_t$	0.01
Soil	Young's module $E_s$ (N/mm <sup>2</sup> )	4.19
	Unit weight $\gamma$ (kN/m <sup>3</sup> )	14.9
	Poisson's Ratio $\nu$	0.4
	Coefficient of earth pressure at rest $K_0$	0.5
	Yield condition	Mohr-Coulomb
	Flow rule	No associated flow
	Cohesion $c$ (N/mm <sup>2</sup> )	0.0008
	Internal friction angle $\phi$ (°)	40
Dilation angle $\psi$ (°)	10	
Pile-Soil	Tangential friction coefficient $f$	0.5

### 3.2. Results of test and FE Analysis

The deformation of meshes under the displacement  $0.3B$  for 4P is shown in Figure 6. The separation between the pile and the soil behind the pile occurred in the analysis, whereas no separation was observed in the test as shown Figure 4(a). The separation was occurred due to the fact that the soil was self-supported because the soil had cohesion slightly in this analysis. In the test, the sand behind the pile flew into this gap between the pile and the soil. It can be interpreted that the analysis can simulate the deformation process of corn shaped hollow.

Distribution of plastic strain for 4P is shown in Figure 7. The plastic strain was concentrated in the soil between two piles. The position of this concentration corresponds to the deformed line by slip shown in Figure 4(b).

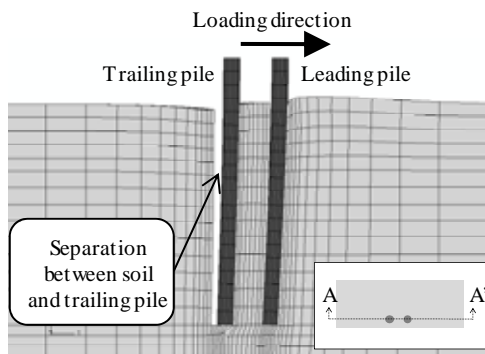


Figure 6 Deformation of mesh by analysis

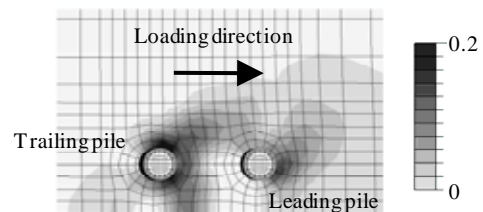


Figure 7 Distribution of plastic strain around pile group (4P)

Figure 8 shows the comparison of the bending moment distribution by analyses and tests. The bending moment distribution for the short pile tests was nearly linear as shown Figure 8(a). On the other hand, the bending moment distribution for the slender pile tests had a maximum under the ground as shown Figure 8(b). The bending moment distribution by analyses can well simulate the test result. Furthermore, the bending moment distribution of the leading pile was close to that of the single pile and was greater than that of the trailing pile. This behavior can be seen in both test results and analysis results.

Figure 9 shows the shear force versus displacement relationship at pile cap. The shear forces by tests were the average of the two sets obtained from the plus and minus directions. The slope of the shear force versus displacement curve rapidly decreased for the test of 4P beyond the displacement at which the pile cap of the

leading pile became full plastic state. This behavior can be seen in both the test and analysis results. Furthermore, the analyses in both short piles and slender piles simulate adequately the difference of shear force between the leading pile and the trailing pile as observed in the test results.

Figure 10 shows the load distribution ratio versus displacement relationship at pile cap. Load distribution ratio is defined as the ratio of the shear force applied on the individual pile to the average load per pile. Average load per pile represents the applied load divided by the number of pile. The load distribution ratio by analysis can well simulate the test result. The load distribution ratio changed from 1.0 as displacement amplitude increase. Furthermore, after the pile cap became full plastic state, the load distribution ratio returned to 1.0 again. This behavior is observed in both short pile case and slender pile case.

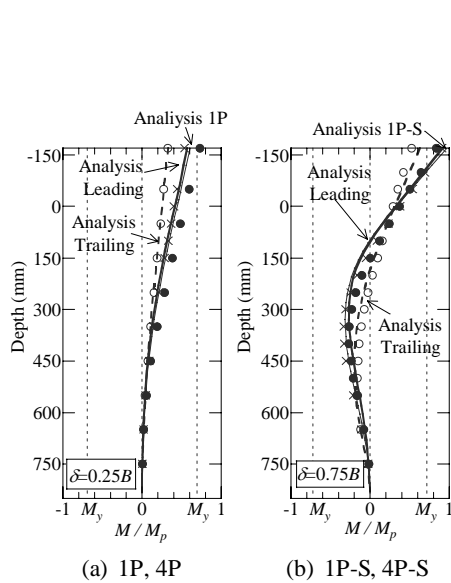


Figure 8 Distribution of bending moment

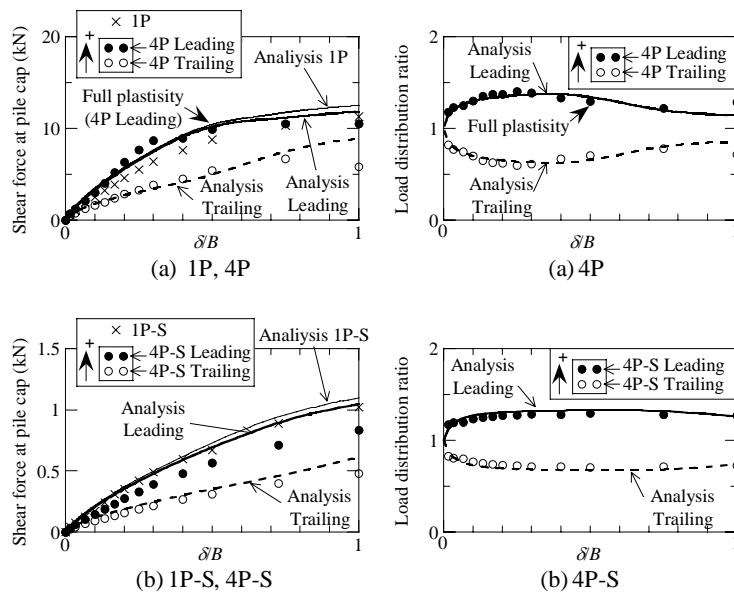


Figure 9 Shear force - displacement relationship at pile cap

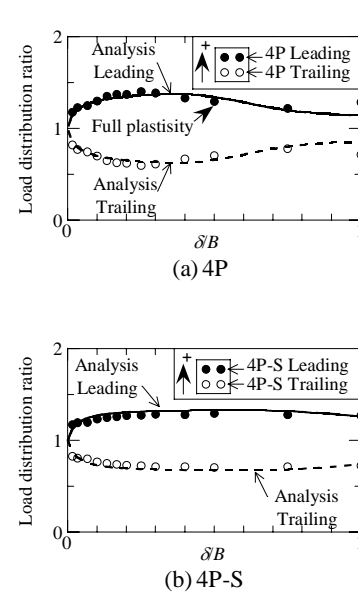


Figure 10 Load distribution ratio - displacement relationship at pile cap

### 3.3. Influence of Nonlinear Behavior of a Pile-Soil Structure on Load Distribution Ratio

Both in the short pile case and slender pile case, the load distribution ratio depends on displacement at the pile cap. The influence of nonlinear behavior of a pile-soil structure on load distribution ratio is investigated about the short pile (4P) in this chapter.

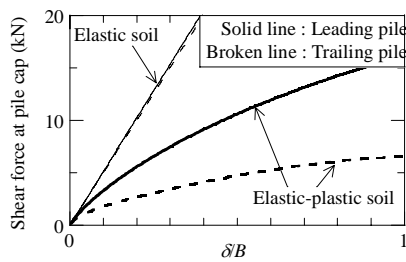
Figure 11 shows the results of analyses by two models about soil, i.e., one was assumed to have Mohr-Coulomb yield condition and the other was assumed to be linear elastic state. Figure 11(a) shows the shear force versus displacement relationship at the pile cap and Figure 11(b) shows the load distribution ratio versus displacement relationship at the pile cap for 4P. The pile was assumed to be linearly elastic in these analyses. The shear force of the leading pile was almost identical with that of the trailing pile in the analysis with the elastic soil. On the other hand, in the analysis with the elastic-plastic soil, the shear force of the leading pile was greater than that of the trailing pile as test results. Furthermore, the load distribution ratio changed from 1.0 by increasing the displacement amplitude as shown in test results until the displacement at which the pile cap became full plastic state.

Since the load distribution ratio substantially changed until the displacement of  $0.1B$ , the nonlinear behavior of soil until the displacement of  $0.1B$  is important. Figure 12 shows the increment distributions of the plastic strain magnitude from the displacement  $0.01B$  to the displacement  $0.1B$  for 4P. The lateral load is applied left-to-right

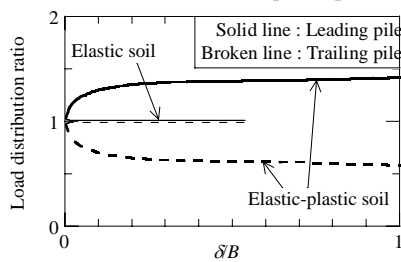
direction in the figure. The failure region of the soil extended with increasing the displacement. As shown in 'X-Y section' of Figure 12, which is the cross section at the depth of 100mm from ground surface, the failure region was concentrated in the soil between two piles under the small amplitude of  $0.01B$  as shown in Figure 4(b) and extended gradually in front of the leading pile. As shown in 'X-Z section' of Figure 12, which is the vertical section through the two piles, the failure region around the trailing pile extended to the deeper area than that around the leading pile. This difference of the extension of the failure area between the leading pile and the trailing pile results in the fact that the load distribution ratio of the leading pile is greater than that of the trailing pile.

Figure 13 shows the results of analyses by two models about pile, i.e., one was assumed to have Mises yield condition and the other was assumed to be linear elastic state. Figure 13(a) shows the shear force versus displacement relationship at the pile cap and Figure 13(b) shows the load distribution ratio versus displacement relationship at the pile cap for 4P. The soil was assumed to have Mohr-Coulomb plastic condition in these analyses. The slope of the shear force versus displacement curve of the leading pile rapidly decreases after the pile cap yielded and the slope of the trailing pile increases. Furthermore, as the pile was assumed to have Mises yield condition, the load distribution ratio returned to 1.0 after the pile cap yielded.

Thus, the analyses can simulate the lateral resistance of pile groups by taking the material nonlinearity of the pile and the soil into account adequately.

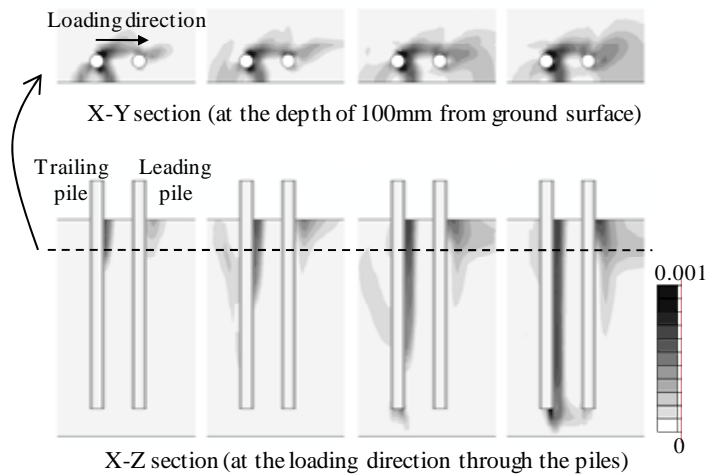


(a) Shear force at pile cap



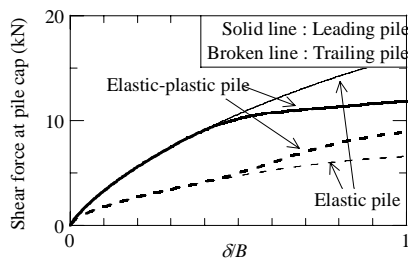
(b) Load distribution ratio

Figure 11 Effects of soil model (4P)

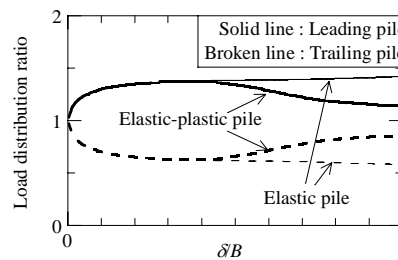


(a)  $\delta = 0.01B$  (b)  $\delta = 0.02B$  (c)  $\delta = 0.05B$  (d)  $\delta = 0.1B$

Figure 12 Distribution of plastic strain increment (4P)



(a) Shear force at pile cap



(b) Load distribution ratio

Figure 13 Effects of pile model (4P)

#### 4. CONCLUSION

To investigate the mechanism of the strong nonlinear behavior of pile-soil structures which is not considered in current seismic design, the cyclic lateral loading tests for the pile group in dry sand subjected extremely large displacement were conducted. Furthermore, elastic-plastic 3-D finite element analyses, in which the pile and the soil were assumed to have the plastic characteristics and the contact boundary condition was considered between the pile and the soil, were performed to obtain better understanding of the tests results. The major findings obtained from this study are summarized as follows; 1) The behavior of the load distribution ratio observed in the tests can be simulated by elastic-plastic 3-D finite element analyses, which were considered about the nonlinear properties in the materials and the contact boundary condition between the piles and the soil. 2) The plastification of the soil and the pile cap remarkably influence the displacement dependency of the load distribution ratio. The plastification of the soil causes the change of the load distribution ratio from 1.0 by increasing the displacement. The plastification of the pile cap in the leading pile causes the return of the load distribution ratio to 1.0 again by increasing the displacement and the increase of shear force at the pile cap in the trailing pile. This behavior is observed in both short pile test and slender pile test.

Thus, the presented analysis model can simulate the lateral resistance behavior of pile groups subjected to large displacement by taking account of the material nonlinearity of the pile and the soil adequately. Especially, the plastification of the pile and the soil has important effect on the load distribution ratio of a pile group. The next subject for a future study is the parametric analysis on the strength of the pile and the soil by using the presented analysis model which evaluate the load distribution ratio and pile group efficiency.

#### REFERENCES

- AIJ. (2001). Recommendations for Design of Building Foundation, AIJ, Tokyo, Japan
- Brown, D. A., Morrison, C., Reese, L. C. (1988). Lateral Load Behavior of Pile Group in Sand. *Journal of Geotechnical Engineering*, ASCE, **114:11**, 1261-1276.
- Kashiwa, H., Kurata, T., Hayashi, Y., Tamura, S., Suita, K. (2007). Displacement amplitude dependence of effect of pile group by cyclic lateral loading tests on large displacement. *Journal of Structural and Construction Engineering Architectural Institute of Japan* **614**, 53-60. (in Japanese)
- Kurata, T., Kashiwa, H., Hayashi, Y., Tamura, S., Suita, K. (2007). Non-linear behavior of pile group-soil system based on horizontal loading test subjected to large displacement. *Journal of Structural and Construction Engineering Architectural Institute of Japan* **614**, 45-52. (in Japanese)
- Saito, H., Tanaka, H., Ishida, T., Koyamada, K., Kontani, O., Miyamoto, Y. (2002). Vibration tests of pile-supported structure in liquefiable sand using large-scale blast. *Journal of Structural and Construction Engineering, the Architectural Institute Japan* **553**, 41-48. (in Japanese)
- Suzuki, Y., Adachi, N. (2003). Relation between subgrade reaction and displacement of model pile group based on horizontal loading test. *Journal of Structural and Construction Engineering, the Architectural Institute Japan* **570**, 115-122. (in Japanese)
- Tatsuoka, F., Goto, S., Sakamoto, M. (1986). Effects of some factors on strength and deformation characteristics of sand at low pressures. *Soil and foundations* **26:1**, 105-114
- Tatsuoka, F. (1993). Introduction to Strength of Soil and Failure of Ground (Third Revision), The Japanese Geotechnical Society. (in Japanese)
- Tominaga, K., Yamamoto, H., Somekawa, J. (1988). Experimental studies on lateral behavior of pile groups under combined load. *Journal of Structural and Construction Engineering, the Architectural Institute Japan* **394**, 130-140. (in Japanese)
- Wakai, A., Gose, S., Ugai, K. (1999). 3-D elasto-plastic finite element analyses of pile foundations subjected to lateral loading. *Soil and foundations* **39:1**, 97-111.